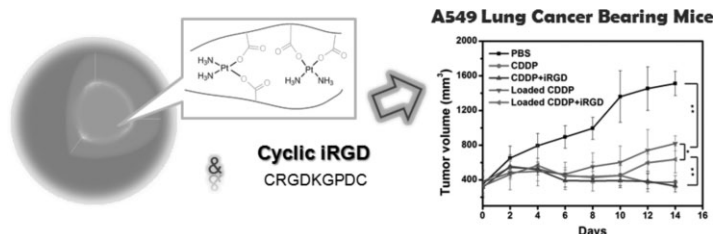


Methoxypoly(ethylene glycol)-*block*-Poly(α -glutamic acid)-Loaded Cisplatin and a Combination With iRGD for the Treatment of Non-Small-Cell Lung Cancers^a

Wantong Song, Mingqiang Li, Zhaohui Tang, Quanshun Li, Yan Yang, Huaiyu Liu, Taicheng Duan, Hua Hong,* Xuesi Chen*

CDDP is loaded into methoxypoly(ethylene glycol)-*block*-poly(α -glutamic acid) (mPEG-*b*-PLG), and a combination with iRGD is applied for NSCLC chemotherapy. The CDDP-loaded micelles show sustained cisplatin release in PBS, dose- and time-dependent inhibition to HeLa and A549 cell proliferation, and no apparent hemolysis activities. In in vivo studies using subcutaneous NSCLC xenograft models (A549), both free CDDP and CDDP-loaded micelles show an evident anti-tumor effect. However, the toxicity of CDDP is significantly reduced in the cases of CDDP-loaded micelles and co-administration with iRGD, and the survival time is prolonged by over 30%. Therefore, mPEG-*b*-PLG-loaded cisplatin and the combination with iRGD provides a promising new therapy for NSCLC.



W. Song, M. Li, Z. Tang, X. Chen

Key Laboratory of Polymer Ecomaterials, Changchun Institute of Applied Chemistry, Chinese Academy of Sciences, Changchun, 130022, P. R. China

E-mail: xschen@ciac.jl.cn

Q. Li, Y. Yang

Key Laboratory for Molecular Enzymology and Engineering of Ministry of Education, College of Life Science, Jilin University, Changchun, 130012, P. R. China

H. Liu, H. Hong

Laboratory Animal Center, Jilin University, Changchun, 130012, P. R. China

E-mail: honghua@jlu.edu.cn

T. Duan

State Key Laboratory of Electroanalytical Chemistry, Changchun Institute of Applied Chemistry, Chinese Academy of Sciences, Changchun, 130022, P. R. China

W. Song, M. Li

Graduate University of Chinese Academy of Sciences, Beijing, 100039, P. R. China

^a Supporting Information is available from the Wiley Online Library or from the author.

W. Song and M. Li contributed equally to this paper.

1. Introduction

Lung cancer has increased to be the world's most common cause of cancer-related death,^[1] and is characterized by highly malignant, invasive growth, and low 5-year survival rates. Small-cell lung cancer (SCLC) and non-small-cell lung cancer (NSCLC) are the two main types of lung cancers based on the characteristics of the disease, and out of which NSCLC accounts for 80% of all lung cancers. NSCLC is a very aggressive lung cancer and has high mortality. Although surgery can offer a chance for a cure when lung cancer is diagnosed in the earlier stages, it is difficult to remove tumor tissue completely in most cases. Thus, chemotherapy is often used for lung cancer, alone or combined with surgery and/or radiation therapy.

Standard first-line therapy for advanced NSCLC consists of platinum-based chemotherapy. *cis*-diamminedichloroplatinum (cisplatin, CDDP), the most effective chemotherapeutic agents, is used to treat 50% of all cancers.^[2] It exerts its antitumor effects by disrupting DNA structure in cell nuclei through the formation of intrastrand and interstrand crosslinks.^[3] Despite the ubiquitous use of

cisplatin in oncology, this drug is associated with significant dose-limiting toxicities including nephrotoxicity and neurotoxicity.^[4] These severe side effects and dose-limiting usage reduce cisplatin's effect in successful cancer treatment.

To improve the therapeutic indices of cisplatin, several new strategies have been developed to decrease the side toxicity and to improve tumor site targeting. Carboplatin and oxaliplatin,^[5] screened from thousands of potent platinum analogues, were proved to be less toxicity. Nanoparticles have been demonstrated to significantly improve drug specificity of action due to nanoparticle-facilitated changes in tissue distribution and pharmacokinetics of drugs.^[6] By encapsulating or incorporating cisplatin in macromolecular carriers, such as water-soluble polymers,^[7] long-circulating liposomes,^[8] and polymeric micelles,^[9] tumor-targetable cisplatin formulations were formed, and favored biodistribution and much lower side effects were proved. NC-6004, developed by Kataoka et al. through coordination of cisplatin to methoxypoly(ethylene glycol)-*block*-poly(L-glutamic acid) (mPEG-*b*-PLG),^[10] had started phase-II clinical trial. Platinum(IV) prodrugs, which act after being reduced to cisplatin(II) intracellularly, and can reduce the toxicity during blood circulation and enhance the cytotoxicity after being endocytosed,^[11] was also developed.

Tumor-targeted delivery of anticancer agents is believed to open a new era to the traditional chemotherapy.^[12] Commonly, drug carriers are modulated with targeting ligands, and tumor sites over expressing the corresponding receptors will ingest much more drugs than other tissues. This has been proved to selectively increase the drug concentration at the tumor site and significantly improve the therapeutic efficacy.^[7b,13] A tumor-penetrating peptide iRGD was reported to increase the vascular and tissue permeability in a tumor-specific and neuropilin-1-dependent manner. The iRGD peptide homes to tumors through a three-step process:^[14] the RGD motif mediates binding to α_v integrins on tumor endothelium and a proteolytic cleavage then exposes a binding motif for neuropilin-1, which mediates penetration into tissue and cells. Thus, when polymer nanoparticles are modified with iRGD, the abilities of tissue penetration and targeting of drug-loaded nanoparticles can be improved.^[15] Besides, this effect cannot only be realized by chemical conjugation, but also by coadministration. It is reported that the therapeutic index of various drugs can be equally improved by systemic injection.^[16]

In this study, mPEG-*b*-PLG-loaded cisplatin and a combination with iRGD was used for the treatment of NSCLC. A549, a cell line that highly expresses α_v integrins^[17] and neuropilin 1 (NRP-1)^[18] and is known for its invasive growth potential,^[19] was used as the NSCLC tumor model.

The novel drug delivery formula was evaluated both in vitro and in vivo in detail.

2. Experimental Section

2.1. Materials

γ -Benzyl-L-glutamate-*N*-carboxyanhydride (BLG-NCA) was synthesized as our previous work.^[20] Amino-terminated poly(ethylene glycol) methyl ether (mPEG-NH₂, $M_w = 5000$ Da) was synthesized according to a literature procedure.^[21] *N,N*-dimethylformamide (DMF) was stored over calcium hydride (CaH₂) and purified by vacuum distillation with CaH₂. Cisplatin was purchased from Shandong Boyuan Chemical Company, China. Cyclic iRGD (CRGDKGPDC) was customized from Apeptide Co. Ltd. (Shanghai, China). All the other reagents and solvents were purchased from Sinopharm Chemical Reagent Co. Ltd. and used as received.

2.2. Synthesis of mPEG-*b*-PLG

mPEG-*b*-PLG was synthesized through the ring-opening polymerization (ROP) of BLG-NCA in DMF using mPEG-NH₂ as initiator. Typically, mPEG-NH₂ (1.0 g, 0.2 mmol) was firstly dehydrated with toluene, then designed amount of BLG-NCA and anhydrous DMF was added. After stirring for 3 d at 25 °C, the solution was precipitated into excess amount of diethyl ether to give the mPEG-*b*-PBLG block copolymers.

Subsequently, mPEG-*b*-PBLG was dissolved in dichloroacetic acid and HBr/acetic acid (33 wt%) was added. The deprotection reaction was conducted at 30 °C for 1 h and then the mixture was precipitated into excessive diethyl ether. After dried under vacuum, the precipitate was dialyzed with distilled water and freeze-dried to give the mPEG-*b*-PLG product.

¹H NMR spectra were recorded on a Bruker AV 400 NMR spectrometer in deuterium oxide (D₂O), or trifluoroacetic acid-*d* (CF₃COOD). Number- and weight-average molecular weights (M_n , M_w) and molecular weight distributions (polydispersity index, $PDI = M_w/M_n$) were determined by means of gel permeation chromatography (GPC) using Waters 515 HPLC pump, with DAWN EOS 18 Angles Laser Light Scattering Instrument and OPTILAB DSP Interferometric Refractometer (Wyatt Technology) as the detector. The eluent was DMF containing 0.01 M lithium bromide (LiBr) or water (phosphate buffer, pH 7.4) at a flow rate of 1.0 mL · min⁻¹. Polystyrene and poly(ethylene glycol) with different molecular weights were used as standard samples respectively.

2.3. Preparation of CDDP-loaded mPEG-*b*-PLG micelles

mPEG-*b*-PLG and CDDP were dissolved in distilled water and reacted at 37 °C for 72 h. Then the mixture was dialyzed in distilled water for 24 h to remove free CDDP. The micelle solution was kept at 4 °C until use. The size distribution of CDDP-incorporated micelles was evaluated by dynamic light scattering (DLS) at 25 °C using a WyattQELS instrument with a vertically polarized He-Ne laser (DAWN EOS, Wyatt Technology) at 90°

collecting optics. Zeta-potentials were measured with a Zeta Potential/BI-90 Plus particle size analyzer (Brookhaven, USA) at room temperature. High-resolution transmission electron microscopy (HRTEM) images were taken from JEOL JEM-1010 TEM with an accelerating voltage of 200 kV. Inductively coupled plasma mass spectrometry (ICP-MS, Xseries II, ThermoScientific, USA) was used for quantitative determination of trace levels of platinum. The drug loading content (DLC %) and drug loading efficiency (DLE %) were calculated according to

$$\text{DLC \%} = \frac{\text{weight of CDDP in micelles}}{\text{weight of drug} - \text{loaded micelles}} \times 100\%$$

$$\text{DLE \%} = \frac{\text{weight of CDDP in micelles}}{\text{total weight of CDDP for loading}} \times 100\%$$

2.4. In vitro Drug Release

The release of the CDDP from the micelles in phosphate-buffered saline (PBS, pH=7.4 and pH=5.5) was evaluated by the dialysis method. Briefly, 5 mL CDDP-incorporated micelles were added to a dialysis membrane tube (molecular-weight cutoff (MWCO)=3500 Da), which was then incubated in 30 mL PBS at 37 °C with a shaking rate of 100 rpm. At predetermined time, 1 mL of incubated solution was taken out and replaced with fresh PBS. The Pt contents of the samples were determined by ICP-MS.

2.5. Cytotoxicity Assay and Cellular Uptake

Two kinds of cells, HeLa and A549 were used to test the in vitro cytotoxicity. HeLa or A549 cells were seeded in 96-well culture plates at a density of 10^4 cells per well in 100 μ L Dulbecco's modified Eagle medium (DMEM) and allowed to attach for 24 h. Then the cells were reseeded with mPEG-*b*-PLG, CDDP or CDDP-incorporated micelles at different concentrations and incubated for another 48 or 72 h. At each time point, cell viability was analyzed using MTT and measured in a Bio-Rad 680 microplate reader at a wavelength of 492 nm.

The following steps were carried out for the cellular uptake studies of A549 cells. A549 cells were seeded in a 6-well culture plate at a density of 2×10^5 cells per well. After attaching for 24 h, CDDP or CDDP-loaded mPEG-*b*-PLG micelles were added into the cultured medium respectively. After incubation for 4 h and 24 h at 37 °C, the medium was removed and rinsed with cold PBS (1 mL \times 3). The cells were trypsinized and cell numbers were counted, then incubated with nitric acid (68 vol%) at 70 °C for 12 h. Platinum content analysis was performed using ICP-MS.

2.6. Hemolysis Assay

Hemolytic activities of pure and CDDP-loaded mPEG-*b*-PLG micelles were assessed by monitoring hemoglobin release from rabbit blood by spectrophotometry. Briefly, freshly obtained blood samples were diluted by physiological saline (PS), and then red blood cells (RBCs) were isolated from serum by centrifugation. After carefully wash and dilution, RBC suspension was added to pure and CDDP-

loaded mPEG-*b*-PLG micelles solution at systematically varied concentrations and mixed by vortex, then kept in static condition at 37 °C for 1 h. Finally, the mixtures were centrifuged and transferred to a 96-well plate. The absorbance values of the supernatants at 540 nm were determined by a Bio-Rad 680 microplate reader. PS (-) and Triton X-100 (10 g \cdot L⁻¹) (+) were used as negative and positive controls, respectively. The hemolysis ratio (HR) of RBCs was calculated using the following formula: hemolysis (%) = $(A_{\text{sample}} - A_{\text{negative control}}) / (A_{\text{positive control}} - A_{\text{negative control}}) \times 100$, where A_{sample} , $A_{\text{negative control}}$ and $A_{\text{positive control}}$ denote the absorbances of samples, negative and positive controls, respectively. All hemolysis experiments were carried out in triplicates.

2.7. Pharmacokinetics

Kunming rats were randomly divided into four groups ($n=3$, average weight 180 g). CDDP, CDDP + iRGD, loaded CDDP, and loaded CDDP + iRGD were administered i.v. via tail vein (3 mg \cdot kg⁻¹ on a CDDP basis, 4 mg \cdot kg⁻¹ iRGD). At defined time periods (3 min, 0.5, 1, 3, 6, 12, and 24 h), blood samples were collected from orbital cavity, heparinized, and centrifuged to obtain the plasma. The plasma samples were decomposed on heating in nitric acid and the Pt contents were measured by ICP-MS.

2.8. In vivo Antitumor Efficiency and Survival Rate

Balb/C nude mice (6 weeks old, male, average body weight 25 g) were purchased from Shanghai and maintained in an SPF (specific pathogen free) class experimental animal room. The mice were randomly divided into five groups ($n=6$) and the human NSCLC xenograft model was established by subcutaneous injection of 1.5×10^6 A549 cells (150 μ L) into the right flank of each mouse. Tumor nodules were allowed to grow to a volume >300 mm³ before initiating treatment. The mice were injected intravenously via tail vein five times at 2 d intervals with free CDDP, CDDP + iRGD, loaded CDDP, loaded CDDP + iRGD (5 mg \cdot kg⁻¹ on a CDDP basis, 4 mg \cdot kg⁻¹ iRGD, 200 μ L of aqueous solution). The control group was administered with PBS. The antitumor activity was evaluated in terms of the tumor size, which was estimated by the following equation: $V = a \times b^2/2$, where a and b were the major and minor axes of the tumors measured by a caliper, respectively. The body weight was measured simultaneously as an indicator of systemic toxicity.

2.9. Biodistribution

Balb/C nude mice were established with human NSCLC xenograft as described above. After the tumor nodules grew to a volume about 300 mm³, loaded CDDP, loaded CDDP + iRGD (5 mg \cdot kg⁻¹ on a CDDP basis, 4 mg \cdot kg⁻¹ iRGD, 200 μ L of aqueous solution) were injected intravenously via tail vein. 6 h later, the mice were sacrificed, and the kidney, liver, spleen, lung, heart, and tumor were excised. The organs were weighted, decomposed on heating in nitric acid, evaporated to dryness, redissolved, and the Pt concentration was measured by ICP-MS.

2.10. Histopathology Evaluation

The histopathology damage evaluation was assessed by hematoxylin and eosin (H-E) method. Briefly, on day 22, mice were anesthetized and the chests were cut open, PBS and paraformaldehyde were perfused from the left atrium. Tumor, liver, and kidney were collected, embedded with paraffin, and cut into 5 μm thickness. The tissues were stained with hematoxylin and eosin to assess histological alterations by microscope (Nikon TE2000U).

2.11. Statistical Analysis

All experiments were performed at least three times and expressed as means \pm SD. Data were analyzed for statistical significance using Student's test. $p < 0.05$ was considered statistically significant.

3. Results and Discussion

3.1. Preparation of the CDDP-Loaded mPEG-*b*-PLG micelles

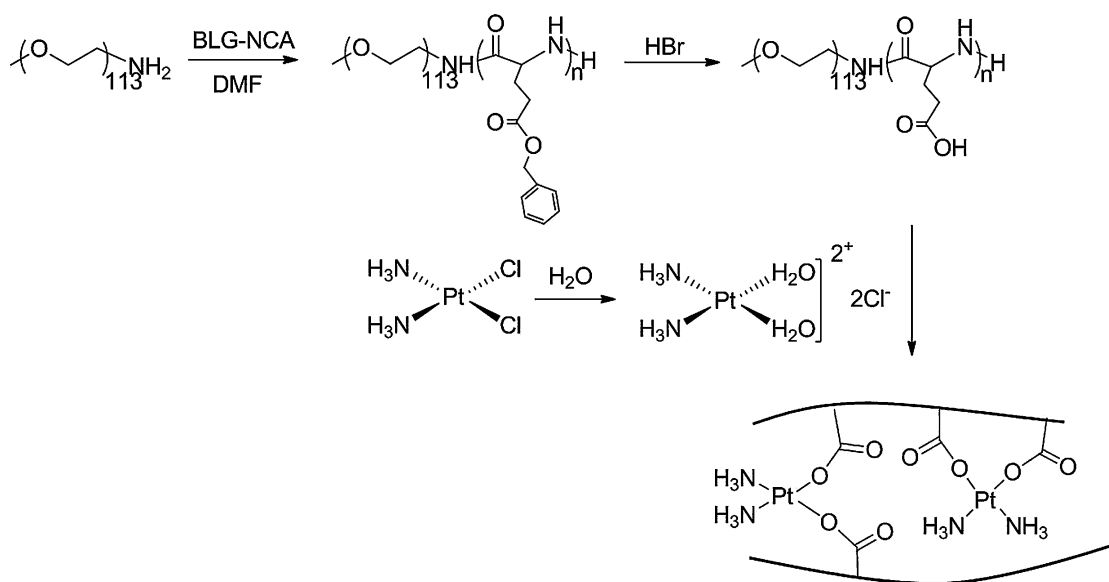
The preparation strategy for CDDP-loaded micelles was shown in Scheme 1. Firstly, mPEG-*b*-PLG copolymer was prepared. Then cisplatin was hydrolyzed and coordinated with the carboxylates of the glutamic acid units to generate CDDP-incorporated micelles.

mPEG-*b*-PLG block copolymer was prepared by the ring-opening polymerization of BLG-NCA using mPEG-NH₂ as the initiator, followed by deprotection of γ -benzyl in HBr/acetic acid. PEG with $\bar{M}_n = 5000$ Da was used, and PLG with 11, 14, 17, 20 segments were synthesized. The ¹H NMR spectra of mPEG-*b*-PBLG₁₁ and mPEG-*b*-PLG₁₁ were shown in Figure S1. The resonances at $\delta = 3.62$ (b) and 3.28 (a) were

attributed to the methylene protons and end methoxy protons of mPEG-CH₂CH₂- (4H and CH₃- (3H), respectively. The resonances at $\delta = 4.2$ (c) were assigned to the protons of the poly(L-glutamic acid) backbone [-C(O)CH(CH₂-)NH-, 1H]. The methylene protons of poly(L-glutamic acid) side groups (-CH-CH₂-CH₂-CO-, 1H, 1H, 2H) gave characteristic signals at $\delta = 1.97$ (d), 2.01 (d) and 2.27 (e). The resonances at $\delta = 5.0$ and 7.1 disappeared in the mPEG-*b*-PLGs, which indicated the complete deprotection of the γ -benzyl groups (C₆H₅-, 5H and C₆H₅CH₂-, 2H).

The \bar{M}_n values of the copolymers before deprotection (mPEG-*b*-PBLG) were determined by GPC using DMF (containing 0.01 M lithium bromide) as the eluent, while after deprotection (mPEG-*b*-PLG), water (phosphate buffer, pH 7.4) was used as the eluent. For mPEG-*b*-PLG, the \bar{M}_n values from GPC were similar to those obtained from ¹H NMR, while the \bar{M}_n values of mPEG-*b*-PBLG from GPC were much larger than those from ¹H NMR. This may be attributed to the existence of secondary structure of polyamino acid in DMF. All the polymers showed narrow molecular weight distribution. The results were listed in Table S1.

The conjugation of the mPEG-*b*-PLG copolymer with CDDP was carried out at 37 °C for 72 h. CDDP was firstly hydrolyzed to cisplatin aqueous complex in distilled water, and then micelles were formed by chelation of Pt(II) with the carboxylates in the copolymers.^[22] The DLC% and DLE% were shown in Figure S2. For mPEG-*b*-PLG₂₀, DLC% had a slightly increase when the COOH/CDDP ratio was increased from 1:0.25 to 1:0.5 (from 16.6 to 23.3%). When the COOH/CDDP ratio was over 0.5, there was no significant change in DLC%. DLE% was decreased with the increase of COOH/CDDP ratio (from 98 to 53%). As the L-glutamic acid units



■ Scheme 1. Preparation of mPEG-*b*-PLG and CDDP complex.

were increased from 11 to 20, no obvious changes were observed in DLC%, while DLE% was decreased from 68.9 to 53.0%. Thus, mPEG-*b*-PLG₁₁ with a COOH/CDDP feed ratio of 0.5 was applied for the following study, and the obtained DLC% and DLE% were 23.4 and 68.9%, respectively.

3.2. Solution Behavior and in vitro Release

TEM micrographs of the CDDP-incorporated micelles are shown in Figure 1. With the incorporation of cisplatin into mPEG-*b*-PLG₁₁, core/shell spherical structure with an average diameter around 15 nm was seen (inset in Figure 1, by HRTEM). The hydrodynamic radii (R_h) measured by DLS was 5–26 nm. The slightly smaller values from TEM observations should be due to the dehydration of the micelles in the TEM sample preparation process. Poly(*L*-glutamic acid) is a negatively charged polymer, thus the zeta potential of the micelles was measured. For mPEG-*b*-PLG₁₁, the zeta potential was -18.21 ± 1.55 mV, while after CDDP incorporation, it increased to -7.82 ± 4.02 mV. The slightly negative charge is quite suitable for in vivo use, which can effectively reduce protein absorbance in blood circulation.^[23]

The in vitro release of the CDDP-incorporated micelles was carried out in PBS (pH = 7.4 and 5.5). The release of CDDP from the complex was due to the inverse ligand exchange reaction of Pt(II) from the carboxylates to the chloride ions in the surroundings in PS,^[7a] as reported by Kataoka et al. As shown in Figure 2, cisplatin was released from the micelles in a controlled and sustained manner, and no initial burst release was observed. This is probably

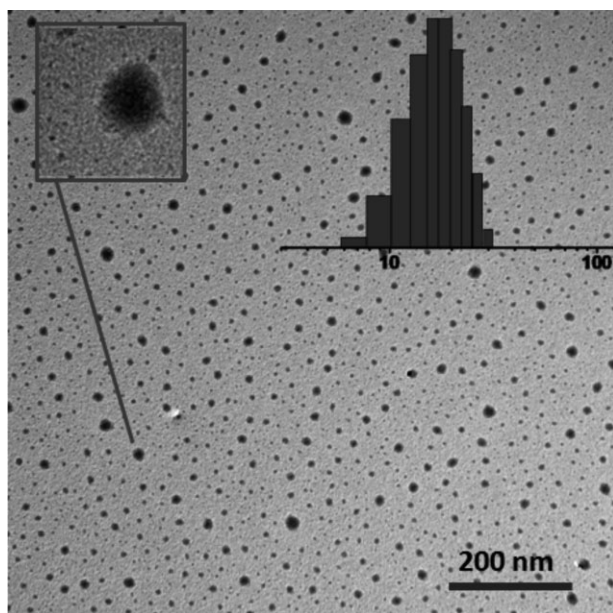


Figure 1. TEM image and DLS characterization of the CDDP-incorporated micelles.

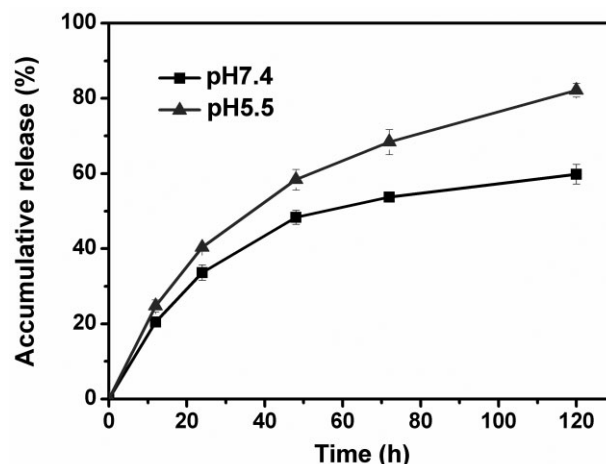


Figure 2. Accumulative release of the CDDP-incorporated micelles in PBS (pH = 7.4 and 5.5). Each point was an average of three measurements.

explained by the strong coordination between CDDP and the carboxylic groups of PLG. What's more, faster drug release was observed at pH = 5.5 than that at pH = 7.4. The accelerated release at acidic pH may be due to the protonation of carboxylic groups of PLG, which weakens the drug and micelles coupling.

3.3. In vitro Cytotoxicity and Endocytosis

The relative cytotoxicity of the materials used for CDDP loading was assessed with a 3-(4,5-dimethylthiazol-2-yl)-2,5-diphenyltetrazolium bromide (MTT) assay. Two cell lines, Henrietta Lacks (HeLa) cells and human lung adenocarcinoma A549 cells were applied. As shown in Figure 3a and c, the viabilities of HeLa and A549 cells treated with mPEG-*b*-PLG₁₁ were all around 80 to 100% at all test concentrations in 48 h, revealing the low toxicity and good compatibility of the copolymer to cells and rendering their potential for efficient drug delivery.

To determine the inhibition of HeLa and A549 cell proliferation in vitro, the cell viabilities were evaluated after 48 or 72 h incubation with CDDP-incorporated micelles, and free CDDP was used as control. As shown in Figure 3b, after 48 h incubation, CDDP-loaded micelles showed dose dependent inhibition for HeLa cell proliferation ($IC_{50} = 24.3 \mu\text{g} \cdot \text{mL}^{-1}$). Figure 3d gave the viability results of A549 cells when incubating with CDDP and CDDP-loaded micelles for 48 and 72 h. Dose and time dependent cell proliferation inhibition was also observed. However, the human lung cancer A549 cells showed much higher tolerance to drugs than that of HeLa cells. After 48 h, CDDP-loaded micelles showed no visible inhibition to A549 cells at a CDDP concentration of $20 \mu\text{g} \cdot \text{mL}^{-1}$. Obvious inhibition was seen only after 72 h ($IC_{50} = 17.0 \mu\text{g} \cdot \text{mL}^{-1}$). The high IC_{50} value of A549 cells was consistent with literature

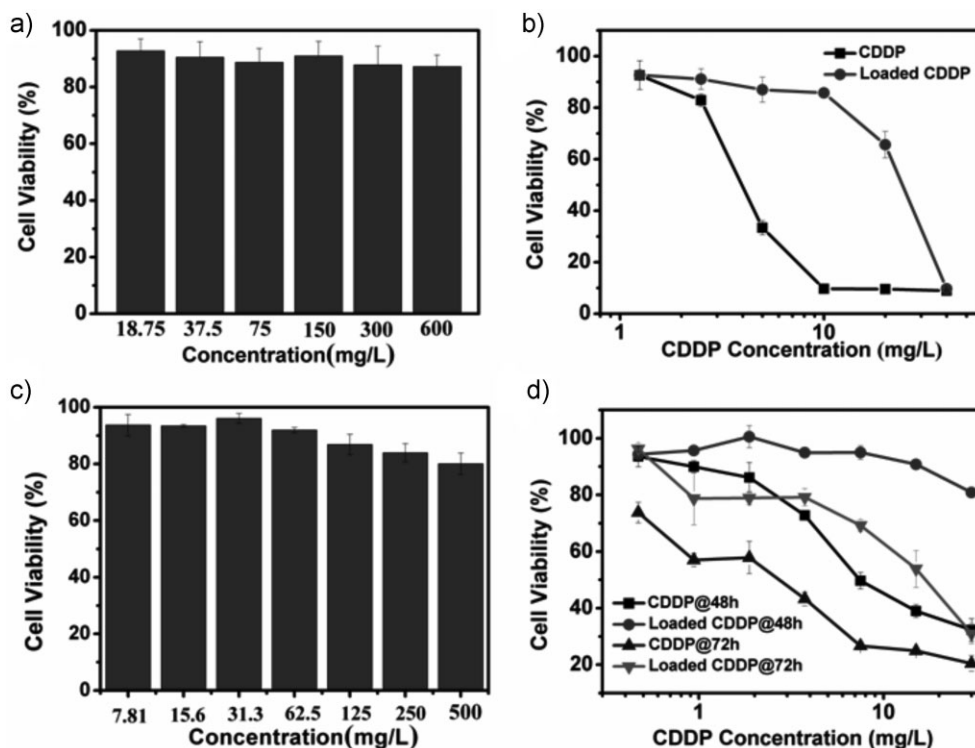


Figure 3. MTT assay with HeLa and A549 cells. (a and c) mPEG-*b*-PLG₁₁ incubated with HeLa and A549 for 48 h; (b) CDDP and loaded CDDP incubated with HeLa for 48 h. (d) CDDP and loaded CDDP incubated with A549 for 48 and 72 h.

results that non-small cell cancer cells lines were relatively non-sensitive to anticancer drugs.^[10,24]

To further investigate the cell proliferation inhibition difference, the endocytosis of free CDDP and CDDP-incorporated micelles into A549 cells was conducted. As listed in Table S2, free CDDP entered tumor cells faster than CDDP-incorporated micelles in the first 4 h. While 24 h later, there were not obvious difference for the CDDP content inside the tumor cells. Thus, the viability differences of free CDDP and CDDP-loaded micelles obtained in Figure 3 should mostly be attributed to the different drug formats. The toxicity of the micelle system acts only after CDDP was dissociated from the complexes, thus the CDDP-incorporated micelles took longer time to reach similar cytotoxicity with free CDDP. This sustained release behavior greatly reduced the toxicity of CDDP, thus higher dosage could be applied and much longer drug effect could be maintained.

3.4. Plasma Clearance

Hemocompatibility is very important for materials used via intravenous injection. The blood compatibilities of mPEG-*b*-PLG₁₁ and CDDP-incorporated micelles were assessed by hemolysis assay on rabbit RBCs. The hemolysis (%) represents the degree of RBC membranes destroyed by substances in contact with RBCs. Smaller value of hemolysis

rate indicates better blood compatibility. As shown in Figure 4a, mPEG-*b*-PLG₁₁ did not show conspicuous hemolytic activities on RBCs even at a very high concentration of 5 mg · mL⁻¹, indicating good hemocompatibility for potential biomedical application. In addition, the hemolytic activities of CDDP-incorporated micelles were established with free CDDP as control. Both the two formats showed no apparent hemolysis activities toward RBCs, which indicated that CDDP-incorporated micelles were hemocompatible allowing the potential clinical applications.

The pharmacokinetics of the different CDDP formats was carried out by tail vein injection into health rats. At predetermined time points, blood was collected and the Pt concentration was tested. Four CDDP formats, CDDP, CDDP + iRGD, loaded CDDP, and loaded CDDP + iRGD were set for blood clearance test. The results were shown in Figure 5. Free CDDP underwent an instant Pt concentration decrease after administration, with <1% left in 3 h. While the loaded CDDP showed remarkably prolonged blood circulation time than the free CDDP formats, with more than 10% left in 10 h. The longer retention time of CDDP-incorporated micelles in blood was reasonably correlated with the inherent enhanced retention effect of the slightly negative micelles with a PEG hydrophilic shell^[23] and the stable sustained release behavior during blood circulation. In addition, by incorporating the CDDP into micelles, the

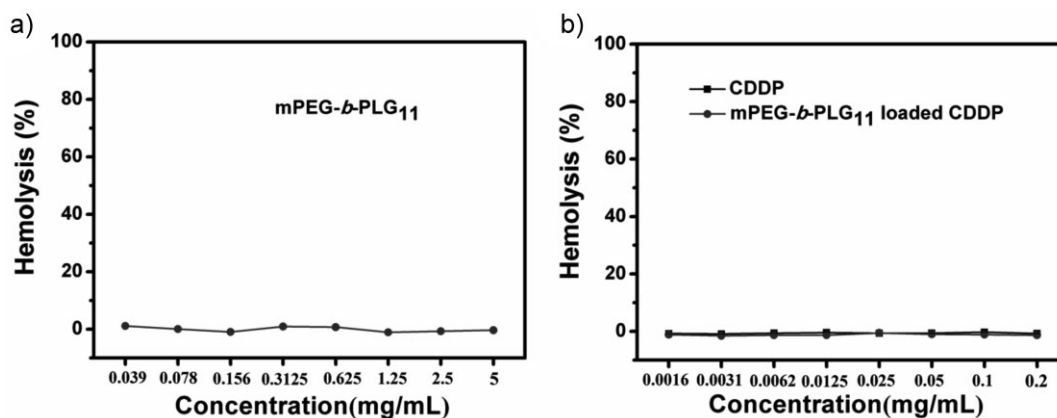


Figure 4. Hemolysis assay of mPEG-*b*-PLG₁₁, CDDP and loaded CDDP. All hemolysis experiments were carried out in triplicates.

chelation of free CDDP to plasma proteins was also greatly reduced. Thus the sustained release and long circulation behavior of the CDDP-incorporated micelles would contribute to the reduction in system toxicity and increased accumulation at the tumor site by the enhanced permeation and retention (EPR) effect.^[25] Coadministration of iRGD did not have much effect on free CDDP metabolism, but slightly enhanced the blood clearance rate for the loaded CDDP group (Figure 5). The accelerated blood clearance rate may be attributed to the “enhanced penetration effect” of the iRGD peptide, as reported in the literature.^[16]

3.5. In vivo Antitumor Efficiency

To explore the antitumor activity of different CDDP formats and the effect of iRGD, BALB/C nude mice subcutaneously

implanted with human lung adenocarcinoma A549 cells were used as the tumor model. Lung cancer is highly malignant and is known for its migration and invasive growth potential. The A549 cells implanted tumor models endured an explosive growing after 21 d latency in nude mice and grew to over 300 mm³ in the following 4 d. Then PBS, free CDDP, CDDP + iRGD, loaded CDDP, and loaded CDDP + iRGD were administered via tail vein at 2 d intervals for five times (5 mg · kg⁻¹ on CDDP basis, 4 mg · kg⁻¹ iRGD). Tumor volumes and body weights were measured at the same time.

The tumor volume measurement results were shown in Figure 6a. Tumors grew very fast in the control group, and increased to over 1500 mm³ in 14 d. The treatment groups all showed obvious tumor inhibition effect during the drug administration period. The four formats had similar antitumor efficiency in the first 6 d. After that, tumors of the loaded CDDP group started to reincrease, while the inhibition effect of the loaded CDDP + iRGD group was continued until day 10. The average tumor volume of mice treated with CDDP-loaded micelles was 820 mm³ on day 14, while when coadministered with iRGD, the volume was about 630 mm³. Free CDDP groups showed continuously tumor regression until we stopped our observation on day 14. However, severe body weight loss also happened from the initial administration (shown in Figure 6b), and this also partially contributed to the tumor volume decrease. In contrast, no body weight loss was observed in groups injected with loaded CDDP. Body weight change is a comprehensive reflection of system toxicity. Clearly, the toxicity of CDDP was evidently reduced after being incorporated into the polymeric micelles.

Figure 7 gave the survival rates of A549 tumor bearing mice of each group. Although mice groups treated with free CDDP had evident effect on tumor inhibition, there was no amelioration on prolonging the survival time of the tumor-bearing mice. In addition, because of severe body toxicity,

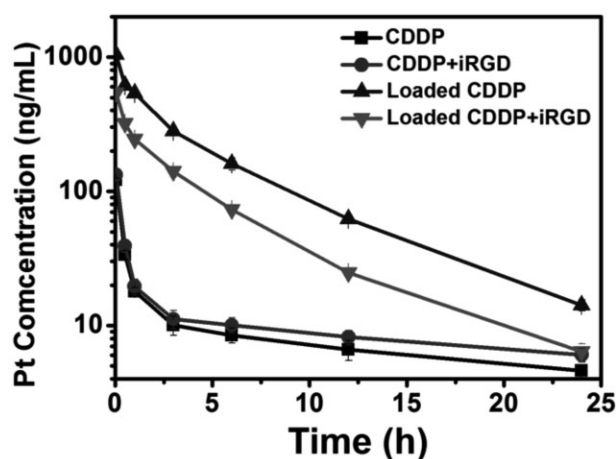


Figure 5. Time profiles of platinum concentration in the plasma after i.v. administration of free CDDP, loaded CDDP and a combination with iRGD. Drugs were administered to healthy rats at a dose of 3 mg · kg⁻¹ based on CDDP, and iRGD at a dose of 4 mg · kg⁻¹. Each group was expressed as mean ± SD (n = 3).

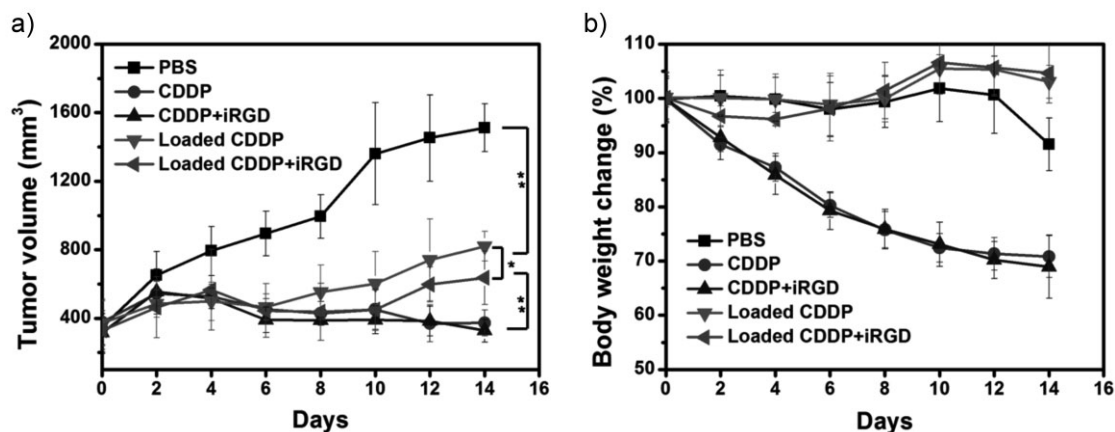


Figure 6. Effect of CDDP formats on anti-tumor efficacy and body weight change of A549 human lung cancer xenograft-bearing nude mice (male). Each drug was administered five times at 2-d intervals (Day 0, 2, 4, 6, 8) at a dose of $5 \text{ mg} \cdot \text{kg}^{-1}$ on a CDDP (iRGD at a $4 \text{ mg} \cdot \text{kg}^{-1}$ dose). The data are shown as mean \pm SD ($n = 6$), * $p < 0.05$, ** $p < 0.01$.

the survival quality was much lowered. Loaded CDDP significantly prolonged the survival time of tumor bearing mice. Death started to appear only at the late stage, about 2 weeks later than the control group. Survival time was also obviously prolonged by combination of loaded CDDP and iRGD. However, slightly earlier death appeared compared with the non-iRGD group.

We further investigated the effect of iRGD on in vivo drug metabolism and distribution. The platinum concentration in kidney, liver, spleen, lung, heart, and tumor was measured 6 h after injection. As shown in Figure S3, after combination with iRGD, drug concentration was increased more or less in every organ. This explained the faster blood clearance rate when iRGD was applied (as shown in Figure 5), and may contribute to the slightly earlier death compared with the non-iRGD group. iRGD was reported to target neo-vascular and increase the penetration ability,^[16]

therefore, drug distribution was slightly increased. However, the drug concentration was much more increased at the tumor site, which still explained the increased anti-tumor effect when iRGD was coadministered.

By combination of the above results, the following conclusions could be made. Free CDDP at doses of $5 \text{ mg} \cdot \text{kg}^{-1}$ caused severe toxicity, and body weight loss appeared since the first treatment. Thus, the continued tumor regression should be partially attributed to the bodyweight loss, and no prolongation in survival time was seen. This severe toxicity greatly cut down the therapeutic window of CDDP in chemotherapy. Loaded CDDP showed obvious anti-tumor efficiency, but the severe toxicity was also significantly reduced since no body weight loss was seen. It was noticeable that by combination with iRGD, loaded CDDP showed an improved anti-tumor effect, which was almost the same as the free CDDP groups during the drug administration period. However, the side effect of CDDP could be significantly reduced by this kind of drug formats. Thus, the therapeutic window was greatly enlarged and higher allowed doses provided opportunities for more effective treatment.

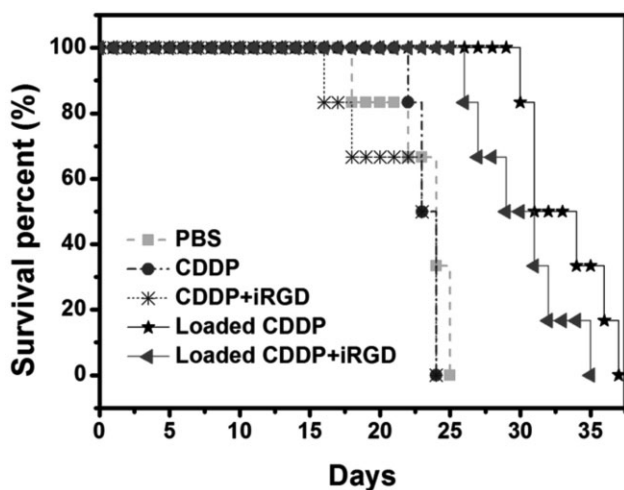


Figure 7. Survival rate of A549 tumor bearing mice that received different CDDP formats.

3.6. Histopathology Evaluation

Tumor curative effect and damage to liver and kidney were further confirmed by histopathological analysis (Figure 8). In normal tissues (A-1), nuclei were stained to be indigo by hematoxylin, while cytoplasm and extracellular matrix were stained to be pink by eosin. Necrotic cells did not have clear cell morphology, and the chromatin became darker or aggregated to goblet or diffused separately outside the cellular. Tumor tissues of all the CDDP treated groups showed obvious cell necrosis, indicating all CDDP formats applied had antitumor effect to A549 lung cancer. Free CDDP treated groups (B-1, C-1) showed the most distinct

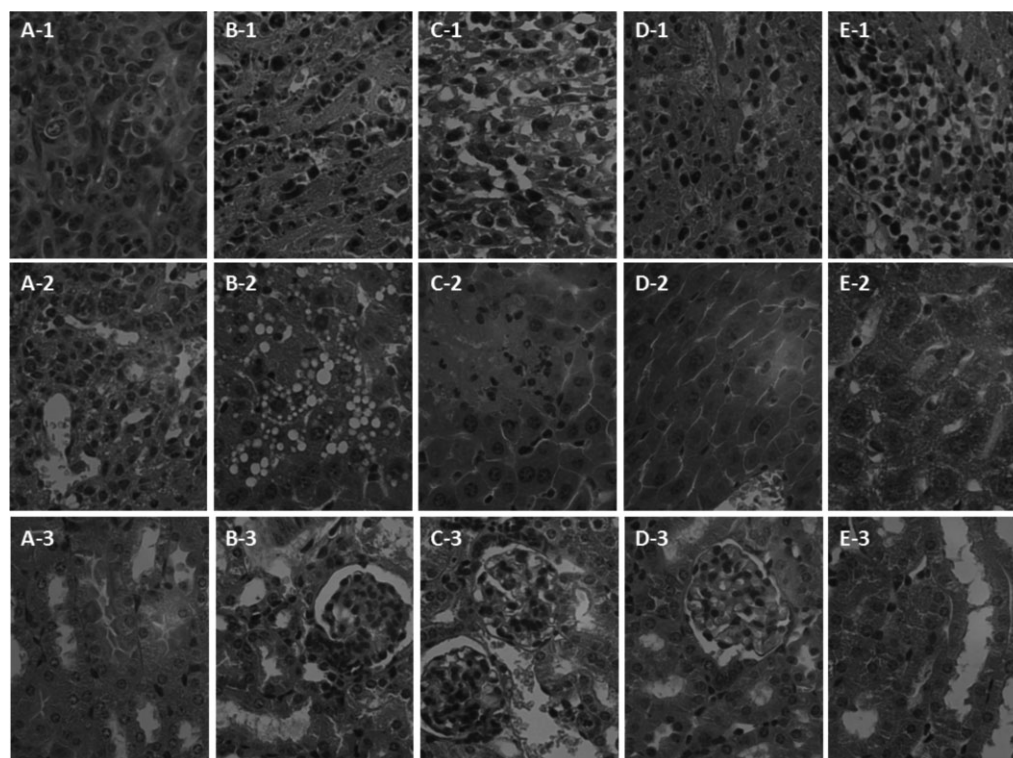


Figure 8. Histopathological analysis of tumor (A-1 to E-1), liver (A-2 to E-2) and kidney (A-3 to E-3) of nude mice bearing A549 tumors on 22 d after treatment with PBS (A), CDDP (B), CDDP + iRGD (C), loaded CDDP (D) and loaded CDDP + iRGD (E).

damage to tumor tissues, as much darker pink color and lack of discernible boundary regions were seen. By combination with iRGD, more severe damage could be seen for the loaded CDDP group (E-1 to D-1), consistent with the tumor volume measurement results. Different morphologies were also observed in liver tissue slices. As listed from A-2 to E-2, loaded CDDP groups showed no damage to liver, while CDDP groups had obvious damage to liver. Surprisingly, more severe injury in liver was seen for the PBS group where the liver cell morphology was almost damaged. Visible damage could also be seen on the liver surface before cutting to slices on day 22. It is reported that the late stages of lung cancer facilitates metastasis to liver,^[26] thus we concluded that migration might happen at the late pathological stages, especially in the non-treatment group. A3 to E3 showed the kidney slices of different groups. Damage was seen in the CDDP treatment groups, while groups treated with loaded CDDP or saline were largely normalized. Severe renal toxicity is the main drawback of CDDP in chemotherapy. These histopathological results showed that the CDDP-loaded micelles could largely reduce the renal toxicity caused by CDDP. In addition, the micelles did not induce any increase in liver toxicity, thus greatly enlarged the therapeutic window of platinum drugs.

4. Conclusion

In this study, mPEG-*b*-PLG-loaded CDDP and a combination with iRGD for the treatment of NSCLC was evaluated in detail. Cisplatin was chelated with the glutamic acid units, and core-shell spherical nanoparticles were formed. The CDDP-loaded micelles showed controlled and sustained cisplatin release in PBS, and dose and time dependent proliferation inhibition to HeLa and A549 cells. In hemolysis assay, both the mPEG-*b*-PLG copolymer and the CDDP-loaded micelles showed no apparent hemolysis activities. When administered in vivo, the CDDP-loaded micelles greatly enhanced the blood circulation time of CDDP. In an in vivo test for A549 lung tumor bearing mice, the combination of mPEG-*b*-PLG-loaded CDDP and iRGD showed similar anti-tumor effect but significantly lower body weight loss in comparison with free CDDP. Therefore, mPEG-*b*-PLG-loaded cisplatin and the combination with iRGD provides a new promising strategy for NSCLC chemotherapy.

Supporting Information

This includes ¹H NMR spectra of mPEG-*b*-PBLG₁₁ and PEG-*b*-PLG₁₁, drug loading content (DLC%) and efficiency (DLE%) of

the series polymers used in this study, tissue distribution of loaded CDDP and loaded CDDP + iRGD after 6 h, number-average molecular weight (\bar{M}_n) and polydispersity index (PDI) of polymers determined by GPC and ^1H NMR, and CDDP and loaded CDDP uptake by A549 cells in 4 and 24 h.

Acknowledgements: We are grateful for financial support from the National Natural Science Foundation of China (20904053, 21074018, 51173184, 51021003), the Ministry of Science and Technology of China (International cooperation and communication program 2010DFB50890 and 2011DFR51090), the Knowledge Innovation Program of the Chinese Academy of Sciences (KJCX2-YW-H19), and the Program of the Science and Technology of Changchun (2010061).

Received: April 24, 2012; Revised: July 11, 2012; Published online: October 15, 2012; DOI: 10.1002/mabi.201200145

Keywords: block copolymers; cisplatin; drug delivery systems; poly(L-glutamic acid); iRGD

- [1] "Cancer", World Health Organization. 2006.
- [2] M. Galanski, M. A. Jakupec, B. K. Keppler, *Curr. Med. Chem.* **2005**, *12*, 2075.
- [3] D. Wang, S. J. Lippard, *Nat. Rev. Drug Discov.* **2005**, *4*, 307.
- [4] D. J. Stewart, C. S. Dulberg, N. Z. Mikhael, M. D. Redmond, V. A. J. Montpetit, R. Goel, *Cancer Chemoth. Pharm.* **1997**, *40*, 293.
- [5] a) M. J. Cleare, *Biochimie* **1978**, *60*, 1038; b) L. M. Pasetto, M. R. D'Andrea, A. A. Brandes, E. Rossi, S. Monfardini, *Crit. Rev. Oncol. Hematol.* **2006**, *60*, 59.
- [6] a) D. Peer, J. M. Karp, S. Hong, O. C. Farokhzad, R. Margalit, R. Langer, *Nat. Nano* **2007**, *2*, 751; b) P. Grodzinski, D. Farrell, K. Ptak, N. J. Panaro, *Pharm. Res.* **2011**, *28*, 273; c) K. Kataoka, A. Harada, Y. Nagasaki, *Adv. Drug Deliv. Rev.* **2001**, *47*, 113; d) W. Wang, J. Ding, C. Xiao, Z. Tang, D. Li, J. Chen, X. Zhuang, X. Chen, *Biomacromolecules* **2011**, *12*, 2466.
- [7] a) N. Nishiyama, S. Okazaki, H. Cabral, M. Miyamoto, Y. Kato, Y. Sugiyama, K. Nishio, Y. Matsumura, K. Kataoka, *Cancer Res.* **2003**, *63*, 8977; b) X.-H. Peng, Y. Wang, D. Huang, Y. Wang, H. J. Shin, Z. Chen, M. Spewak, H. Mao, X. Wang, Y. Wang, Z. Chen, S. Nie, D. Shin, *ACS Nano* **2011**; c) V. T. Huynh, G. Chen, P. de Souza, M. H. Stenzel, *Biomacromolecules* **2011**, *12*, 1738.
- [8] S. Khiati, D. Luvino, K. Oumzil, B. Chauffert, M. Camplo, P. Barthélémy, *ACS Nano* **2011**, *11*, 8649.
- [9] a) X. Li, R. Li, X. Qian, Y. Ding, Y. Tu, R. Guo, Y. Hu, X. Jiang, W. Guo, B. Liu, *Eur. J. Pharm. Biopharm.* **2008**, *70*, 726; b) G. Mattheolabakis, E. Taoufik, S. Haralambous, M. L. Roberts, K. Avgoustakis, *Eur. J. Pharm. Biopharm.* **2009**, *71*, 190; c) N. V. Nukolova, H. S. Obero, S. M. Cohen, A. V. Kabanov, T. K. Bronich, *Biomaterials* **2011**, *32*, 5417.
- [10] H. Uchino, Y. Matsumura, T. Negishi, F. Koizumi, T. Hayashi, T. Honda, N. Nishiyama, K. Kataoka, S. Naito, T. Kakizoe, *Br. J. Cancer* **2005**, *93*, 678.
- [11] a) S. Dhar, F. X. Gu, R. Langer, O. C. Farokhzad, S. J. Lippard, *Proc. Natl. Acad. Sci. USA* **2008**, *105*, 17356; b) S. Dhar, N. Kolishetti, S. J. Lippard, O. C. Farokhzad, *Proc. Natl. Acad. Sci. USA* **2011**, *108*, 1850; c) H. H. Xiao, R. G. Qi, S. Liu, X. L. Hu, T. C. Duan, Y. H. Zheng, Y. Huang, X. Jing, *Biomaterials* **2011**, *32*, 7732; d) J. Yang, W. Liu, M. Sui, J. Tang, Y. Shen, *Biomaterials* **2011**, *32*, 9136.
- [12] a) P. M. Valencia, M. H. Hanewich-Hollatz, W. Gao, F. Karim, R. Langer, R. Karnik, et al., *Biomaterials* **2011**, *32*, 6226; b) Z. Xiao, E. Levy-Nissenbaum, F. Alexis, A. Lupták, B. A. Teply, J. M. Chan, J. Shi, E. Digga, J. Cheng, R. Langer, O. C. Farokhzad, *ACS Nano* **2012**, *6*, 696.
- [13] a) W. Wang, D. Cheng, F. Gong, X. Miao, X. Shuai, *Adv. Mater.* **2012**, *24*, 115; b) A. Eldar-Boock, K. Miller, J. Sanchis, R. Lupu, M. J. Vicent, R. Satchi-Fainaro, *Biomaterials* **2011**, *32*, 3862; c) X. Jiang, X. Sha, H. Xin, L. Chen, X. Gao, X. Wang, K. Law, J. Gu, Y. Chen, Y. Jiang, X. Ren, Q. Ren, X. Fang, *Biomaterials* **2011**, *32*, 9457.
- [14] K. N. Sugahara, T. Teesalu, P. P. Karmali, V. R. Kotamraju, L. Agemy, O. M. Girard, D. Hanahan, R. F. Mattrey, E. Ruoslahti, *Cancer Cell* **2009**, *16*, 510.
- [15] a) Z. Zhu, C. Xie, Q. Liu, X. Zhen, X. Zheng, W. Wu, R. Li, Y. Ding, X. Jiang, B. Liu, *Biomaterials* **2011**, *32*, 9525; b) H. T. Zhang, H. C. Li, Z. W. Li, C. H. Guo, *Anticancer Drugs* **2011**, *22*, 409.
- [16] K. N. Sugahara, T. Teesalu, P. P. Karmali, V. R. Kotamraju, L. Agemy, D. R. Greenwald, E. Ruoslahti, *Science* **2010**, *328*, 1031.
- [17] A. Schutz, W. Hartig, M. Wobus, J. Grosche, C. Wittekind, G. Aust, *Virchows Arch.* **2005**, *446*, 421.
- [18] P. Frankel, C. Pellet-Mary, P. Lehtolainen, G. M. D'Abaco, M. L. Tickner, L. L. Cheng, I. C. Zachary, *EMBO Rep.* **2008**, *9*, 983.
- [19] H. Wang, W. L. Fu, J. H. Im, Z. Y. Zhou, S. A. Santoro, V. Iyer, C. M. DiPersio, Q. C. Yu, V. Quaranta, A. Al-Medhi, R. J. Muschel, *J. Cell Biol.* **2004**, *164*, 935.
- [20] H. Y. Tian, C. Deng, H. Lin, J. R. Sun, M. X. Deng, X. S. Chen, X. Jing, *Biomaterials* **2005**, *26*, 4209.
- [21] M. S. Thompson, T. P. Vadala, M. L. Vadala, Y. Lin, J. S. Riffle, *Polymer* **2008**, *49*, 345.
- [22] N. Nishiyama, K. Kataoka, *J. Controlled Release* **2001**, *74*, 83.
- [23] K. Xiao, Y. P. Li, J. T. Luo, J. S. Lee, W. W. Xiao, A. M. Gonik, R. G. Agarwal, K. S. Lam, *Biomaterials* **2011**, *32*, 3435.
- [24] a) H. Y. Tsai, C. C. Chiu, P. C. Lin, S. H. Chen, S. J. Huang, L. F. Wang, *Macromol. Biosci.* **2011**, *11*, 680; b) V. T. Huynh, G. J. Chen, P. de Souza, M. H. Stenzel, *Biomacromolecules* **2011**, *12*, 1738; c) H. Wang, Y. Zhao, Y. Wu, Y. L. Hu, K. H. Nan, G. J. Nie, H. Chen, *Biomaterials* **2011**, *32*, 8281.
- [25] a) X.-M. Sun, J.-x. Xu, J.-B. Tang, M.-H. Sui, Y.-q. Shen, *Chin. J. Polym. Sci.* **2011**, *29*, 427; b) V. Torchilin, *Adv. Drug Deliv. Rev.* **2011**, *63*, 131.
- [26] H. Kikkawa, M. Kaihou, N. Horaguchi, T. Uchida, H. Imafuku, A. Takiguchi, Y. Yamazaki, C. Koike, R. Kuruto, T. Kakiuchi, H. Tsukada, Y. Takada, N. Matsuura, N. Oku, *Clin. Exp. Metastasis* **2002**, *19*, 717.